Solvent effects in time-dependent self-consistent field methods. I. Optical response calculations

J. A. Bjorgaard,[1,a)] V. Kuzmenko,[2] K. A. Velizhanin,[3] and S. Tretiak[4,b)]
[1]*Center for Nonlinear Studies, Theoretical Division, Los Alamos National Laboratory, Los Alamos, New Mexico 87545, USA*
[2]*National Technical University of Ukraine, KPI, 37 Peremogy Avenue, Building 7, Kiev 03056, Ukraine*
[3]*Theoretical Division, Los Alamos National Laboratory, Los Alamos, New Mexico 87545, USA*
[4]*Center for Integrated Nanotechnologies, Center for Nonlinear Studies, and Theoretical Division, Los Alamos National Laboratory, Los Alamos, New Mexico 87545, USA*

(Received 31 October 2014; accepted 29 December 2014; published online 22 January 2015)

We implement and examine three excited state solvent models in time-dependent self-consistent field methods using a consistent formalism which unambiguously shows their relationship. These are the linear response, state specific, and vertical excitation solvent models. Their effects on energies calculated with the equivalent of COSMO/CIS/AM1 are given for a set of test molecules with varying excited state charge transfer character. The resulting solvent effects are explained qualitatively using a dipole approximation. It is shown that the fundamental differences between these solvent models are reflected by the character of the calculated excitations. © *2015 AIP Publishing LLC.* [http://dx.doi.org/10.1063/1.4905828]

I. INTRODUCTION

Solvent can have a drastic effect on molecular chromophores,[1] yet modeling the excited state (ES) properties of solute-solvent systems comprises a difficult task for quantum chemistry.[2] A full quantum mechanical (QM) treatment of a solute in a solvent is prohibitively expensive for most methods. Instead, a hybrid method involving a QM approach for the solute and simplified molecular mechanical (MM)[3] or continuum[4] approach for the solvent can be used. These methods are well established for ground state (GS) electronic structure calculations using self-consistent field (SCF) methods, e.g., Hartree-Fock (HF) and Density Functional Theory (DFT) methods, but additional complexity is involved when performing optical response calculations and for determining the ES electronic structure of the solute. Time-dependent self-consistent field (TD-SCF) methods of calculating the ES electron density require both a GS and ES calculation. In both GS and ES calculations, the effects of mutual polarization of the solute and solvent system can be important.[5] For the ES, this polarization involves the ES electron density, which complicates the TD-SCF equations. Much work has gone into developing methods to take this mutual polarization into account. Developed methods involve different relationships between solvent effects in the GS and ES.[6–8] A clear comparison between these methods is necessary for future developments.[5,9]

A discussion of solvent effects in TD-SCF calculations is naturally preceded by a description of the potential of the solvent. Two main approaches for calculating this potential are the QM/MM and continuum (implicit) approach. The advantage of QM/MM is that it includes the explicit molecular structure of the solvent. Effects such as hydrogen bonding and viscosity can be taken into account. However, accurate calculations require averaging over many configurations such that the calculation can become prohibitively expensive. Alternatively, an implicit definition of the solvent is possible. These simulate dielectric effects by treating the solvent as a continuum and, in a sense, averaging over the many possible solvent configurations. In continuum approaches, the solute is modeled as a system embedded in a dielectric cavity.[4] This problem is solved using electrostatics such that the system-environment interaction is mediated by an environment dielectric constant. In this case, the Coulomb interactions in the solute Hamiltonian are effectively screened by the cavity polarization caused by the solute charge density. This is the general idea behind implicit solvent methods when applied to electronic structure calculations.

Several variations of implicit solvent exist[4,10–12] such that the method of cavity surface discretization and/or the method of calculating the charge distribution of the cavity can vary. Perhaps most popular is the polarizable continuum model (PCM) which uses a self-consistent reaction field.[12] A faster method is the conductor-like screening method (COSMO)[13] or similarly the conductor-like PCM (CPCM).[11] In this method, the ideal cavity charges are determined directly from a single system of linear equations at each iteration of the SCF calculation. In contrast, determining the cavity charges in PCM is more complex and computationally demanding, not only involving solution of a system of linear equations but also, in its original form, expensive iteration. When the state of interest is the GS, calculation with these methods is straightforwardly performed with the GS charge density. For ES calculations, mutual polarization requires calculations with the solute ES charge density and becomes more complex.

Mutual polarization in QM/MM methods is similar. A term describing the polarization of the solvent molecules is

a)Electronic mail: jbjorgaard@lanl.gov
b)Electronic mail: serg@lanl.gov

calculated from the solute charge density and solvent charges. Including this mutual polarization of QM and MM partitions requires that the solute charge density and solvent polarization terms be determined self-consistently.[14] The resulting terms in the calculation of the solute charge density are similar to the PCM/CPCM potential, differing only in the method of calculating the solvent charges. Therefore, properly including an effective solvent potential in ES electronic structure calculations is necessary for both QM/MM and implicit solvent methods. This can involve iterative solution of the GS and TD-SCF equations.

Even without solvent effects, ES calculations for optical molecules are more complex than GS calculations due to the importance of many-body interactions, i.e., electronic correlations, in the ES. Many methods have been developed to accurately treat these interactions. Among the simplest and computationally efficient, the time-dependent HF method (TD-HF) has been in use for many decades.[15,16] Over the last decade, it was expanded to include hybrid HF/DFT models resulting in the TD-SCF method. The TD-SCF method includes many specific flavors ranging from time-dependent DFT (TD-DFT) to TD-HF. They have become the most popular methods for calculating optical properties of nano-sized materials, with new hybrid functionals still being developed to more accurately treat electron correlation and empirically reproduce experimental results.[17–19]

The working equations of TD-SCF methods in the frequency domain are the random-phase approximation (RPA) eigenvalue equations. They involve the eigenvalues of a tetradic matrix of dimension $N^2 \times N^2$ where N is the number of basis functions. The formal numerical cost of diagonalization scales as $O(N^6)$ because of the RPA matrix dimensions. Effective Krylov subspace algorithms and iterative diagonalization techniques have been developed (e.g., Davidson algorithm).[20–27] These approaches are able to efficiently calculate the portion of the eigenspectrum of the RPA matrix necessary for modeling electronic excitations (i.e., the lower portion of the eigenspectrum). Such diagonalizers are common in most modern quantum-chemical codes. This allows efficient computation of excited state properties for molecular systems, generally reaching $O(N^2) - O(N^4)$ complexity. Utilizing sparse algebra techniques, $O(N)$ scaling for excited state calculations have become possible in the atomic orbital basis.[28–37] A number of recent efforts have been devoted to the development of linear-scaling orbital-free algorithms for calculation of excited states and dynamic (hyper) polarizabilities.[38–44]

Here, we concentrate on including solvent effects in optical response calculations using the RPA equations in the molecular orbital basis, but formulations in the atomic orbital basis are straightforward. In vacuum, the GS molecular orbitals are calculated self-consistently with the GS charge density using, i.e., the standard HF or DFT methods. To include a solvent model, modification of the Fock or Kohn-Sham matrix and the RPA eigenvalue equation is necessary. Upon addition of an effective potential that depends on the ES density to the RPA eigenvalue equation and/or the GS Fock or Kohn-Sham matrix, the RPA eigenvalue equation becomes nonlinear. Iterative solution including both the GS SCF and RPA eigenvalue equation is then necessary with self-consistency occurring in the ES charge density and effective solvent potential. Since this involves the choice of a specific state to form the solvent potential, it is described as state-specific (SS).[7,45] It is important to note that the variational principle of the GS SCF equations is not necessarily applicable when a potential dependent on the excited state density matrix is added to the GS Fock or Kohn-Sham matrix.

On the other hand, it is possible to formulate the effective solvent potential in a linear response (LR) scheme[6,46,47] where the RPA eigenvalue problem remains linear so that iterative solution is not necessary. Despite the computational simplicity of the LR scheme, the lack of effects from the ES density matrix provides drastically different results. Intermediate schemes referred to as the vertical excitation model (VE)[48] and corrected LR (cLR) model[8] have also been developed. In the VE model, the effective solvent potential in the GS depends only on the GS density matrix, but in the ground to ES transitions it depends on the ES density matrix.[48] The VE model can be thought of as being SS in the excitation calculation and similarly solved self-consistently with iteration only over the RPA eigenvalue equation. The cLR model is essentially a single iteration of the VE model using a relaxed excited state density and has similar properties, but is not a self-consistent method. The VE model has become well used in excited state coupled cluster theories[49–52] where its analytical gradient is available.[50] The SS model referred to in the following involves calculation of both the GS and ES density matrices with an effective potential depending on the total ES density matrix.

It is also important to consider nonequilibrium effects in solvation models. Molecular chromophores typically display spectral shifts which depend on solvent effects. This shift is typically referred to as solvatochromism. Solvatochromism may have different magnitude in the absorption and emission spectra. The result is a solvent mediated Stokes shift. This can be explained by invoking separation of solvent degrees of freedom into fast and slow partitions.[53] The fast degrees of freedom are assumed to reorganize instantaneously with changes in the solute electrostatic potential, while the slow degrees of freedom are frozen in a configuration reflecting to the GS density. A time dependent reorganization of the slow degrees of freedom then occurs so that at long times, both fast and slow partitions respond to the ES density. These two situations have been described as nonequilibrium and equilibrium solvation, respectively.[7,45] The extension of the equations given below to nonequilibrium solvation involves a partitioning of the effective solvent potential into GS and ES parts. These terms are then scaled by the static and optical dielectric constants, respectively. In this manuscript, we discuss only the equilibrium case in order to focus on a comparison of solvent model effects, while nonequilibrium solvation may become more complex in dynamic simulations.

The aim of this paper is to implement existing ES solvation models in the TD-SCF framework in a unifying manner to clearly compare their effects. In Sec. II, the TD-SCF framework in the RPA representation is formulated with an effective solvent potential. This demonstrates the approximations made to arrive at LR, SS, and VE models. In Sec. III, we apply these methods to a set of test systems which

have excitations with varying charge transfer (CT) character. By comparison with the dipole approximation, we show the solvent effects which are native to each model and discuss their appropriateness for describing specific types of excitations. Conclusions are summarized in Sec. IV.

II. THEORETICAL METHODOLOGY

A. TD-SCF framework

To introduce the TD-SCF theory spanning TD-HF[16,54] and adiabatic TD-DFT[55,56] approaches, we start from a von-Neumann-type equation of motion of a single-electron density matrix which is obtained by a variation of the GS density matrix $\boldsymbol{P}$, $\boldsymbol{\mathcal{P}}(t) = \boldsymbol{P} + \delta\boldsymbol{P}(t)$[57]

$$i\frac{\partial \boldsymbol{\mathcal{P}}}{\partial t} = [\boldsymbol{F}(\boldsymbol{\mathcal{P}}), \boldsymbol{\mathcal{P}}] + [\boldsymbol{R}(t), \boldsymbol{\mathcal{P}}], \tag{1}$$

where $\boldsymbol{F}(\boldsymbol{\mathcal{P}})$ is the effective single-particle Hamiltonian, i.e., the Fockian (or the Kohn-Sham Hamiltonian in DFT) and $\boldsymbol{R}(t)$ is an external perturbation (e.g., induced by an external optical field). Square brackets denote the usual fermionic commutator, $[\boldsymbol{A}, \boldsymbol{B}] = \boldsymbol{AB} - \boldsymbol{BA}$. For brevity, here and everywhere, we assume an orthogonal representation, i.e., an orthogonal AO basis is defined, for instance, by Löwdin decomposition of the overlap matrix $\boldsymbol{S}$.[58]

The first-order response to the perturbation $\boldsymbol{R}(t)$ under variation of the density matrix $\delta\boldsymbol{P}(t)$ contains information about observables such as the frequency-dependent responses. This first-order response is given by

$$i\frac{\partial \delta\boldsymbol{P}}{\partial t} = \mathbb{L}(\boldsymbol{\delta P}) + [\boldsymbol{R}(t), \boldsymbol{P}], \tag{2}$$

where

$$\mathbb{L}(\boldsymbol{x}) \equiv [\boldsymbol{F}(\boldsymbol{P}), \boldsymbol{x}] + [\boldsymbol{G}(\boldsymbol{x}), \boldsymbol{P}] \tag{3}$$

is a tetradic Liouville super-operator[23,57] acting on an arbitrary density matrix $\boldsymbol{x}$, and $\boldsymbol{G}(\boldsymbol{x})$ is the Coulomb-exchange operator. In the frequency domain, the time-dependent evolution of $\boldsymbol{\mathcal{P}}(t)$ can be expanded via eigensolutions of $\mathbb{L}$ when the perturbations $\boldsymbol{R}(t)$ are weak. This is a typical strategy for finite molecular systems. Alternatively, $\boldsymbol{\mathcal{P}}(t)$ can be obtained by propagating Eq. (2) directly in real-time,[59–62] an approach common in solid-state physics and in the limit of strong fields.[63–65]

In the general framework applicable to TD-HF, adiabatic TD-DFT techniques or their hybrid mixture,[66,67] the matrix elements of the Fock (or Kohn-Sham) operator $\boldsymbol{F}(\boldsymbol{x})$ are given by

$$F_{ij\sigma}(\boldsymbol{x}) = t_{ij\sigma} + J_{ij\sigma}(\boldsymbol{x}) - K_{ij\sigma}(\boldsymbol{x}) + v^{xc}_{ij\sigma}(\boldsymbol{x}), \tag{4}$$

where the Coulomb and HF exchange terms are represented as

$$J_{ij\sigma}(\boldsymbol{x}) - K_{ij\sigma}(\boldsymbol{x}) = \sum_{kl\sigma'}(ij\sigma \mid kl\sigma')P_{kl\sigma'} - c_x(ik\sigma \mid jl\sigma')P_{kl\sigma}\delta_{\sigma\sigma'}. \tag{5}$$

Here, indices i, j, k, l, and σ refer to the spatial orbitals and the spin space, respectively. $t_{ij\sigma}$ are one-electron integrals accounting for the kinetic energy and nuclear attraction of an electron, and $(ij\sigma|kl\sigma')$ are conventional two-electron integrals representing Coulombic interactions. The exchange-correlation potential v^{xc}, given by a functional derivative of the exchange-correlation action A^{xc} in the DFT approach,[55,56,68] vanishes in HF theory. The hybrid mixing parameter c_x accounts for the amount of Hartree-Fock exchange in $\boldsymbol{F}(\boldsymbol{P})$. This parameter allows interpolation between pure DFT ($c_x = 0$) and Hartree-Fock ($c_x = 1$ and $A^{xc} = 0$) theories. The total Coulomb-exchange term is defined as

$$G_{ij\sigma}(\boldsymbol{x}) = J_{ij\sigma}(\boldsymbol{x}) - K_{ij\sigma}(\boldsymbol{x}) + \sum_{kl\sigma'} f^{xc}_{ij\sigma,kl\sigma'}x_{kl\sigma'}, \tag{6}$$

where the f^{xc} kernel is a functional derivative of the exchange-correlation potential v^{xc} in the DFT approach. Note that in Eqs. (4)–(6), the indices i, j, k, l, and σ run over all basis functions $\{\chi(\boldsymbol{r})\}$ irrespectively of representation. If the GS density matrix is calculated from a single Slater determinant, i.e., HF or DFT, it fulfills the condition

$$[\boldsymbol{F}(\boldsymbol{P}), \boldsymbol{P}] = 0. \tag{7}$$

B. RPA eigenproblem

The eigenspectrum of the Liouville operator $\mathbb{L}$ in Eq. (3) is given by the $N^2 \times N^2$ eigenvalue problem

$$\mathbb{L}\vec{v} = \Omega\vec{v}, \tag{8}$$

where the vector $\vec{v}$ is dyadic, corresponding to the unrolled $N \times N$ matrix $\boldsymbol{v}$, i.e., $\boldsymbol{v}_{N\times N} \Leftrightarrow \vec{v}_{N^2\times 1}$, where the double-headed arrow denotes both equivalence and a tensorial mapping.[69]

Traditionally, molecular orbitals provide a convenient representation allowing trivial decomposition of all possible transitions among occupied (hole, h) and virtual (particle, p) orbitals. A complete eigenspectrum of $\mathbb{L}$ in Eq. (8) thus includes two distinct classes of transitions, interband (ph,hp) and intraband (pp,hh). Only "through-gap" electronic excitations related to the interband transitions are of interest for modeling spectroscopic observables.[23] The kth eigenvector of Eq. (8), v_k, corresponds to the variation of density at some frequency Ω. The eigenvalues Ω represent vertical transition energies from the GS to an ES, entering as the poles of the linear response function of the system (see Eq. (2)). For the kth transition, one can write an ES density matrix for ES k such that $\boldsymbol{\mathcal{P}}_k = \boldsymbol{P} + \boldsymbol{v}_k$. Further, the eigenvectors $\vec{v}$ can be decomposed into interband ($\boldsymbol{\xi}$) and intraband ($\boldsymbol{T}$) parts,

$$\boldsymbol{v} = \boldsymbol{\xi} + \boldsymbol{T} = \begin{pmatrix} \boldsymbol{0} & \boldsymbol{Y} \\ \boldsymbol{X} & \boldsymbol{0} \end{pmatrix} + \begin{pmatrix} \boldsymbol{T}^{pp} & \boldsymbol{0} \\ \boldsymbol{0} & \boldsymbol{T}^{hh} \end{pmatrix}, \tag{9}$$

where the index k is dropped for convenience.

The single electron density matrix given in Eq. (1) is required to be idempotent at all times, i.e., $\boldsymbol{\mathcal{P}}^2 = \boldsymbol{\mathcal{P}}$. This leads to a straightforward relationship between the inter- and intraband components of $\boldsymbol{v}$. When $\boldsymbol{v}$ is small, $\boldsymbol{T}$ is given to second order in $\boldsymbol{\xi}$ by[70,71]

$$\boldsymbol{T} = \frac{1}{2}[[\boldsymbol{\xi}^T, \boldsymbol{P}], \boldsymbol{\xi}]. \tag{10}$$

If the GS density matrix in the molecular orbital basis has the block structure

$$\boldsymbol{P} = \begin{pmatrix} \boldsymbol{I} & 0 \\ 0 & 0 \end{pmatrix}, \tag{11}$$

it can be written in the molecular orbital basis as

$$\boldsymbol{T}^{hh} = -\boldsymbol{T}^{pp} = \boldsymbol{X}^2 + \boldsymbol{Y}^2. \tag{12}$$

Matrix $\boldsymbol{T}$ is referred to as the unrelaxed difference density matrix. It is unrelaxed because when added to $\boldsymbol{P}$ it describes a nonvariational solution for the ES density matrix. A variational solution for the ES density matrix can be determined with further calculation by using the Z-vector technique.[71,72] This will be discussed in the context of solvent models in a follow-up publication. Using Eq. (12), it is possible to construct the full $N \times N$ matrix $\boldsymbol{\mathcal{P}}_k$ from the kth eigenvector of the interband partition of $\mathbb{L}$.

Since the inter- and intraband components of the density matrix are related, we can use a reduced space of $\mathbb{L}$ and determine the eigenspectrum of the interband partition, solving for the eigenvectors $\begin{pmatrix} \vec{X} \\ \vec{Y} \end{pmatrix}$. Consequently, Eq. (8) is frequently recast in the MO representation as

$$\begin{pmatrix} \boldsymbol{A} & \boldsymbol{B} \\ -\boldsymbol{B} & -\boldsymbol{A} \end{pmatrix} \begin{pmatrix} \vec{X} \\ \vec{Y} \end{pmatrix} = \Omega \begin{pmatrix} \vec{X} \\ \vec{Y} \end{pmatrix}, \tag{13}$$

which is known as the RPA eigenvalue equation.[73–76]

Submatrices $\boldsymbol{A}$ and $\boldsymbol{B}$ are 4th-order tensors, i.e., they have a super-operator structure defined on the Liouville space $(N_{occ}N_{virt}) \times (N_{occ}N_{virt})$. Here, N_{occ} and N_{virt} denote the Hilbert spaces of occupied and virtual molecular orbitals, respectively, with $N = N_{occ} + N_{virt}$. The tetradic elements of these matrices can always be chosen to be real. They are given in the canonical MO basis as[56,71,77]

$$\begin{aligned} A_{ia\sigma,jb\sigma'} &= (\varepsilon_{a\sigma} - \varepsilon_{i\sigma})\delta_{ij}\delta_{ab}\delta_{\sigma\sigma'} + (ia\sigma \mid jb\sigma') \\ &\quad + f_{ia\sigma,jb\sigma'} - c_x(ab\sigma \mid ij\sigma)\delta_{\sigma\sigma'}, \end{aligned} \tag{14}$$

$$\begin{aligned} B_{ia\sigma,jb\sigma'} &= (ia\sigma \mid jb\sigma') + f_{ia\sigma,jb\sigma'} \\ &\quad - c_x(ja\sigma \mid ib\sigma)\delta_{\sigma\sigma'}, \end{aligned} \tag{15}$$

where indices i, j (a, b) run over occupied (virtual) molecular orbitals, ε_a and ε_i denote energies of molecular orbitals (Fockian eigenvalues), and the other quantities have been introduced in Eqs. (5) and (6).

In Eq. (13), matrices $\boldsymbol{A}$ and $\boldsymbol{B}$ are Hermitian. Matrix $\boldsymbol{A}$ is identical to the Configuration Interaction Singles (CIS) matrix. Neglecting $\boldsymbol{B}$, diagonalization of $\boldsymbol{A}$ gives the CIS excitation energies for a HF Hamiltonian, while for a DFT Hamiltonian, it is known as the Tamm-Dancoff approximation (TDA).[73,78,79] Matrix $\boldsymbol{A}$ is a diagonally dominant matrix for typical molecules. The first term of $\boldsymbol{A}$ in Eq. (14) is equivalent to the first term for the Liouville operator in Eq. (3). It gives a zero order approximation to the excitation energies. If only this part is included in $\mathbb{L}$, the eigenvalues of Eq. (8) are simply the energy differences between the single-particle excitation energies, e.g., Fockian eigenvalues. The rest of the elements of $\boldsymbol{A}$ and $\boldsymbol{B}$ (i.e., the second term for the Liouville operator in Eq. (3)) are additional Coulomb and exchange-correlation screening of the excitation process.

The eigensolutions of Eq. (13) have a paired structure due to the J-symmetry of $\mathbb{L}$ in the interband subspace

$$\mathbb{L}\vec{\xi}_\alpha^+ = \Omega_\alpha \vec{\xi}_\alpha^+, \quad \mathbb{L}\vec{\xi}_\alpha^- = -\Omega_\alpha \vec{\xi}_\alpha^-, \tag{16}$$

where $\alpha = 1, \ldots, N_{occ} \times N_{virt}$ and the matrix transpose relates positive and negative transition density matrices (eigenvectors) $\boldsymbol{\xi}_\alpha^- = (\boldsymbol{\xi}_\alpha^+)^T$, which can always be chosen as real values. These paired eigensolutions of Eq. (13) (or Eq. (8) in the interband *ph, hp* subspace) correspond to excitation and de-excitation processes across the gap, which may be optically activated. The $\vec{X}$ and $\vec{Y}$ components of the eigenvector $\vec{\xi}^+ = \begin{pmatrix} \vec{X} \\ \vec{Y} \end{pmatrix}$ $\left(\vec{\xi}^- = \begin{pmatrix} \vec{Y} \\ \vec{X} \end{pmatrix}\right)$ in the MO representation are, respectively, the particle-hole (*ph*) and hole-particle (*hp*) components. For a majority of molecules, the $\vec{X}$ component dominates (i.e., $\|\vec{X}\| \gg \|\vec{Y}\|$) because elements of super-matrix $\boldsymbol{B}$ represent higher-order electronic correlations and their magnitudes are small compared to those of matrix $\boldsymbol{A}$. Consequently, the TDA ($\boldsymbol{B} = 0$, $\vec{Y} = 0$) is considered as a good approximation and is widely used for the original RPA problem.

C. Solvent effects in TD-SCF methods

This description of ES solvation in TD-SCF methods begins with the LR model. The formulation of solvent effects is then extended to give the SS and VE models in Subsections II C 1 and II C 2. The Fock matrix of a molecule in vacuum (Eq. (4)) is modified by addition of an effective solvent potential $\boldsymbol{V}_S(\boldsymbol{x})$,[6] e.g., defined explicitly for COSMO in the Appendix,

$$\boldsymbol{F}_{LR}(\boldsymbol{x}) = \boldsymbol{F}(\boldsymbol{x}) + \boldsymbol{V}_S(\boldsymbol{x}), \tag{17}$$

where $\boldsymbol{F}_{LR}(\boldsymbol{x})$ is the modified Fock operator. Instead of obeying Eq. (7), the HF or Kohn-Sham GS now fulfills the condition $[\boldsymbol{F}_{LR}(\boldsymbol{P}), \boldsymbol{P}] = 0$.

Replacing the Fock matrix in Eq. (1) with Eq. (17) produces an additional term in Eq. (3). The result is a modified Liouville operator

$$\mathbb{L}_{LR}(\boldsymbol{x}) \equiv [\boldsymbol{F}_{LR}(\boldsymbol{P}), \boldsymbol{x}] + [\boldsymbol{G}(\boldsymbol{x}), \boldsymbol{P}] + [\boldsymbol{V}_S(\boldsymbol{x}), \boldsymbol{P}]. \tag{18}$$

Partitioning the $\boldsymbol{\mathcal{P}}$ as described in Sec. II B to produce an RPA eigenvalue equation (Eq. (8)) results in the modification of Eqs. (14) and (15),

$$A^{LR}_{ia\sigma,jb\sigma'} = A_{ia\sigma,jb\sigma'} + \langle ia\sigma|\hat{V}^S_{ia\sigma,jb\sigma'}|jb\sigma'\rangle, \tag{19}$$

$$B^{LR}_{ia\sigma,jb\sigma'} = B_{ia\sigma,jb\sigma'} + \langle ia\sigma|\hat{V}^S_{ia\sigma,jb\sigma'}|jb\sigma'\rangle, \tag{20}$$

where $\hat{V}^S_{ia\sigma,jb\sigma'}$ are the matrix elements of a tetradic operator describing the solvent effects. The molecular orbital energies in $\boldsymbol{A}$ come from diagonalization of $\boldsymbol{F}_{LR}(\boldsymbol{P})$, i.e., GS solvent effects are present in the Fockian eigenvalues.

This results in a LR solvent model. In the latter two parts of this section, it is shown that the VE and SS models result from relaxing the procedure of partitioning and linearization of the transition density when a Fock matrix modified by an effective solvent potential is used in the equation of motion for $\boldsymbol{\mathcal{P}}$ (Eq. (1)).

Combining Eqs. (16) and (12). The effect of LR solvent on the transition energy can be written as

$$\Delta\Omega_{LR} = Tr(\boldsymbol{T}\boldsymbol{V}_S(\boldsymbol{P})) + Tr(\boldsymbol{\xi}^T\boldsymbol{V}_S(\boldsymbol{\xi})), \tag{21}$$

while the effect of LR solvent on the GS energy is

$$\Delta E_{LR} = Tr(\boldsymbol{P}\boldsymbol{V}_S(\boldsymbol{P})). \quad (22)$$

Equations (21) and (22) should not be mistaken for solvation energies. The solvation energy is related to the difference between the energies in vacuum and solution.[80] The transition and GS densities will be different for systems in solvent and vacuum so that Eqs. (21) and (22) do not correspond to well known observables. Yet, they are still a measure of the magnitude of the solvent effect in the solvated system and are used in Sec. III to compare solvent effects between the models.

1. State specific model

To produce a SS model, we first rewrite the Fock matrix to include the effective solvent potential of the kth solvated ES $\boldsymbol{\mathcal{P}}_k$

$$\boldsymbol{F}_{SS}(\boldsymbol{x}, \boldsymbol{\mathcal{P}}_k) = \boldsymbol{F}(\boldsymbol{x}) + \boldsymbol{V}_S(\boldsymbol{\mathcal{P}}_k). \quad (23)$$

At this point, it is important to note that Eq. (23) includes the use of both inter- and intraband components of $\boldsymbol{\mathcal{P}}_k$. However, in the following, we neglect the interband component to compare with other formulations.[7,9] The intraband partition is given by $\bar{\boldsymbol{\mathcal{P}}}_k = \boldsymbol{P} + \boldsymbol{T}_k$. Nonetheless, it has been suggested that including the interband component might lead to a more accurate treatment.[9] Here, $\bar{\boldsymbol{\mathcal{P}}}_k$ must be treated differently from $\boldsymbol{\mathcal{P}}$ such that it is not linearized in the first order response function (Eq. (3)) and creates a nonlinear term. The LR Liouville operator is

$$\mathbb{L}_{SS}(\boldsymbol{x}) \equiv [\boldsymbol{F}_{SS}(\boldsymbol{P}, \bar{\boldsymbol{\mathcal{P}}}_k), \boldsymbol{x}] + [\boldsymbol{G}(\boldsymbol{x}), \boldsymbol{P}]. \quad (24)$$

Compared with Eq. (3), only one additional term enters Eq. (24), $[\boldsymbol{V}_S(\bar{\boldsymbol{\mathcal{P}}}), \boldsymbol{x}]$, which is represented in Eqs. (14) and (15) by modification of the molecular orbital energies and structures calculated using Eq. (23) rather than Eq. (4). The GS is calculated in the SS model by iteration involving diagonalization of $\boldsymbol{F}_{SS}$, solution of the kth eigenvector of $\mathbb{L}_{SS}$, and calculation of $\bar{\boldsymbol{\mathcal{P}}}_k$.

The effect of SS solvent on the transition energy is then given by

$$\Delta\Omega_{SS} = Tr(\boldsymbol{T}\boldsymbol{V}_S(\bar{\boldsymbol{\mathcal{P}}}_k)) \quad (25)$$

while the effect on the GS energy is

$$\Delta E_{SS} = Tr(\boldsymbol{P}\boldsymbol{V}_S(\bar{\boldsymbol{\mathcal{P}}}_k)). \quad (26)$$

The effect of solvent on the ES energy is then $\Delta\Omega_{SS} + \Delta E_{SS} = Tr(\bar{\boldsymbol{\mathcal{P}}}\boldsymbol{V}_S(\bar{\boldsymbol{\mathcal{P}}}_k))$, where the lack of index denotes that $\bar{\boldsymbol{\mathcal{P}}}$ refers to any state. We note that the entire spectrum of excitation energies obtained from this approach (as well as the VE model) can be defined within the effective potential of a single specific ES. This may find application in, e.g., the calculation of nonlinear optical properties[70] or nonadiabatic dynamics by surface hopping methods[81] for solvated molecules.

2. Vertical excitation model

A related method is obtained when the separation of $\bar{\boldsymbol{\mathcal{P}}}_k$ into ground and excited parts occurs differently for the GS and ES calculations. The GS is calculated using the LR Fock operator (Eq. (17)) while the VE Liouville operator becomes

$$\mathbb{L}_{VE}(\boldsymbol{x}) \equiv [\boldsymbol{F}_{LR}(\boldsymbol{P}), \boldsymbol{x}] + [\boldsymbol{G}(\boldsymbol{x}), \boldsymbol{P}] + [\boldsymbol{V}_S(\boldsymbol{T}_k), \boldsymbol{x}]. \quad (27)$$

Here, an artificial separation of the GS and ES parts of $\bar{\boldsymbol{\mathcal{P}}}_k$ is performed for the GS so that the GS density matrix has no dependence on the ES. Part of the solvent term in Eq. (27) is not contained in the Fock operator (Eq. (17)) and appears explicitly in Eq. (27), yet the total solvent term is $[\boldsymbol{V}_S(\boldsymbol{\mathcal{P}}_k), \boldsymbol{x}]$ because $\boldsymbol{V}_S(\boldsymbol{P})$ enters from Eq. (17) in Eq. (27) (here we assume $\boldsymbol{V}_S(\boldsymbol{x}_A) + \boldsymbol{V}_S(\boldsymbol{x}_B) = \boldsymbol{V}_S(\boldsymbol{x}_A + \boldsymbol{x}_B)$). In a RPA formulation, Eqs. (14) and (15) are straightforwardly modified

$$A^{VE}_{ia\sigma,jb\sigma'} = A_{ia\sigma,jb\sigma'} + V_S(\boldsymbol{T}_k)_{ji\sigma}\delta_{ab} - V_S(\boldsymbol{T}_k)_{ab\sigma}\delta_{ij}, \quad (28)$$

$$B^{VE}_{ia\sigma,jb\sigma'} = B_{ia\sigma,jb\sigma'} + V_S(\boldsymbol{T}_k)_{ji\sigma}\delta_{ab} - V_S(\boldsymbol{T}_k)_{ab\sigma}\delta_{ij}. \quad (29)$$

The effect of solvent on the transition energy is then given by Eq. (25), but the obtained transition density is different so that the magnitude of the solvent effect is different for SS and VE methods. We designate the solvent effect given by Eq. (25) for the VE model as $\Delta\Omega_{VE}$. The effect of solvent on the GS energy is identical to the LR model in Eq. (22).

D. Computational details

For numerical tests of the three outlined solvent models, we use a semiempirical CIS/AM1 technique,[23,82–84] which allows us to consider realistic large molecular systems and mimic the calculations performed with large scale first principles codes. All numerical tests are based on the Collective Electronic Oscillator (CEO) code.[23,82–84] This package combines commonly used semiempirical models (such as AM1, PM3, INDO/S) with RPA and CIS formalisms. The ES calculations are in practice no more computationally demanding the GS calculations using this method, so molecular systems up to thousands of atoms are routinely possible. The CEO modeling of electronic spectra has been successfully applied in the past to calculate optical properties of a variety of conjugated chromophores, e.g., polymers, dendrimers, biological light-harvesting complexes, and carbon nanotubes.[23,82–86] It has been extended to model non-adiabatic dynamics in electronically excited systems.[81,87] Solvent models have NOT been included in these methods to date. The implementation of solvent models in the CEO program may be extended to include solvent effects in nonadiabatic dynamics.

The COSMO effective potential is implemented using a standard scheme, given generally in the Appendix. The Fockian and two-electron integrals in the RPA equation are calculated using a semiempirical AM1[88] scheme in the CEO program.[23] For the ground state, standard self-consistent solution of a GS Fockian[88] is performed. Then, for the LR model, several eigenvectors of the Liouville operator are found. For SS and VE models, iterative solution of the GS Fockian and/or Liouville operator with substitution of $\bar{\boldsymbol{\mathcal{P}}}_k$ from the previous step is performed. This iterative procedure continues until convergence is achieved in the total energy $(E_{gr} + \Omega_k)$ for the state k. For the calculations presented here, convergence is achieved at a difference of 10^{-7} eV in the total energy between iterations.

At each iteration, reordering of the calculated transitions is possible. To follow the correct state k through the self-consistent calculation, the overlap between the transition densities from the current step and the transition density for state k from the previous step is calculated. Then, k is changed to follow the state of highest overlap with the previous step. It is occasionally necessary to tune a linear mixing parameter λ such that the solvent potential is calculated from a linear combination of the previous densities, i.e., such that the solvent potential at step n is given by $\boldsymbol{V}_S(\lambda\bar{\boldsymbol{P}}_n + (1-\lambda)\bar{\boldsymbol{P}}_n)$ where n is used to denote the iteration number. This slows the convergence so that the overlap between transitions at different iterations is increased, making it easier to follow the transition densities when they change rapidly between iterations.

A test set of two bichromophoric CT systems[89] (**1**,**2**), a prototypical chromophore with a single π system (**3**), and a π-stacked CT dimer[90] (**4**/**5**) were used to inspect excitations with various degrees of CT character. These systems exhibit excitations with π-π^*, intramolecular CT, and intermolecular CT character. For comparison, all molecular geometries were optimized on the GS potential energy surface without solvent effects. The dimer of **4**/**5** was prepared by arranging the optimized molecular geometries such that the π systems were aligned in parallel at a reasonable separation of 2.5 Å and the molecular centers of mass were aligned in the coordinates perpendicular to the separation vector (Fig. 1).

III. COMPARISON OF LR, VE, AND SS

A comparison of SS and LR models in TDDFT has been performed by Corni and Cammi *et al.*[9,91] while Caricato *et al.* compared the VE and LR models in TDDFT[8] and between SS and LR models in coupled cluster methods.[92,93] In the original formulation of the VE model by Marenich *et al.*, all available excited state solvation models were compared with experimental benchmarks for accuracy.[48] Here, we perform a detailed comparison of the SS, VE, and LR models using a range of dielectric constants. Our formalism allows us to approximately describe the effects of different models within a dipole approximation to aid in discussion of the relationship between these solvation models. We use COSMO with the same dielectric constant for GS and ES calculations (the formulation of the effective solvent potential and function of the dielectric constant are given in the Appendix). This corresponds to equilibrium solvation for SS and VE models.[7] Within the LR model, this may also be considered equilibrium solvation, even though the relaxation of the ES density is not described.[9]

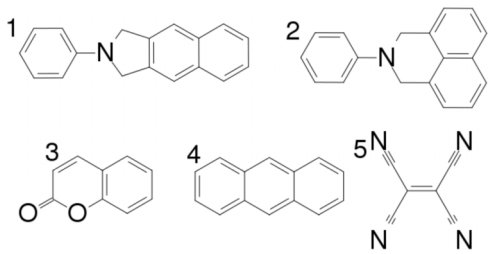

FIG. 1. Chemical structures of molecules used in this study.

By denoting the dipole moment of an arbitrary density matrix $\boldsymbol{x}$ as $\vec{\mu}_{\boldsymbol{x}} = Tr(\hat{\mu}\boldsymbol{x})$ where $\hat{\mu}$ is the dipole operator, we can write the dipole approximation of Eqs. (21) and (25). In the dipole approximation, the equilibrium solvent effect on the transition energy is approximately proportional to

$$\Delta\Omega_{LR} \propto \vec{\mu}_{\boldsymbol{T}} \cdot \vec{\mu}_{\boldsymbol{P}} + \vec{\mu}^2_{\boldsymbol{\xi}} \tag{30}$$

for LR and

$$\Delta\Omega_{SS(VE)} \propto \vec{\mu}_{\boldsymbol{T}} \cdot \vec{\mu}_{\boldsymbol{P}} + \vec{\mu}_{\boldsymbol{T}} \cdot \vec{\mu}_{\boldsymbol{T}_k} \tag{31}$$

for SS or VE. A similar approximation for the effect on the GS energy can be written as

$$\Delta E_{LR(VE)} \propto \vec{\mu}^2_{\boldsymbol{P}} \tag{32}$$

for LR or VE and

$$\Delta E_{SS} \propto \vec{\mu}^2_{\boldsymbol{P}} + \vec{\mu}_{\boldsymbol{P}} \cdot \vec{\mu}_{\boldsymbol{T}_k} \tag{33}$$

for SS. The following results will be discussed in the context of these equations in order to arrive at clear picture of the qualitative differences between LR, VE, and SS models. First, we describe a previously published model comparison.

For comparison of transition energies resulting from SS and LR models, Corni *et al.*[9] used an analytic four-state model (two solvent and two solute states) to arrive at conclusions regarding the differences in predicted solvent effects. They noted that the SS model accounted for only the correlated relaxation of the solvent with respect to the ES electronic wavefunction, e.g., $\vec{\mu}_{\boldsymbol{T}} \cdot \vec{\mu}_{\boldsymbol{T}_k}$, while the LR model accounted only for dispersion interactions, e.g., $\vec{\mu}^2_{\boldsymbol{\xi}}$. Both of these effects were present in their general calculation for the four-state model such that both SS and LR correspond to a different approximation of the full solvent effect.

The results in Eqs. (30) and (31) are nearly identical to the analytical formulation by Corni *et al.* but include the term $\vec{\mu}_{\boldsymbol{T}} \cdot \vec{\mu}_{\boldsymbol{P}}$. The physical interpretation of this term is the effective electrostatic interaction of the GS with the change in electron density in the ES. Here, it is the result of the effective solvent potential from the GS density matrix in the Fock operator. This was not included in the simplified analytical model and is not necessary to explain the differences between LR and SS models.

By inspection of Fig. 2, one can immediately identify transitions which exhibit the character of the three interactions present in Eqs. (30) and (31). For example, transition 1 of Fig. 2(b) and transition 2 of Fig. 2(a) exhibit pronounced $\vec{\mu}^2_{\boldsymbol{\xi}}$ effects since there is a large solvent shift in the LR method, but not in SS or VE models. Similarly, transitions 1 and 4 in Fig. 2(d) exhibit pronounced $\vec{\mu}_{\boldsymbol{T}} \cdot \vec{\mu}_{\boldsymbol{T}_k}$ effects. One can immediately recognize these as CT states, with substantial movement of charge in the ground to ES transition resulting in large $\vec{\mu}_{\boldsymbol{T}} \cdot \vec{\mu}_{\boldsymbol{T}_k}$. Transition 4 in Figs. 2(a) and 2(b) may exhibit $\vec{\mu}_{\boldsymbol{T}} \cdot \vec{\mu}_{\boldsymbol{P}}$ effects because the solvent shifts for SS, VE, and LR methods are significant. This was confirmed by checking the gas phase dipole moments and it must be noted that effects from the other two types of interactions are also partially involved in these solvent shifts. Further, the solvent shifts of the SS and VE models are significantly different.

The origin of this discrepancy can be traced to the effect of the solvent model on the GS. The magnitude of this effect

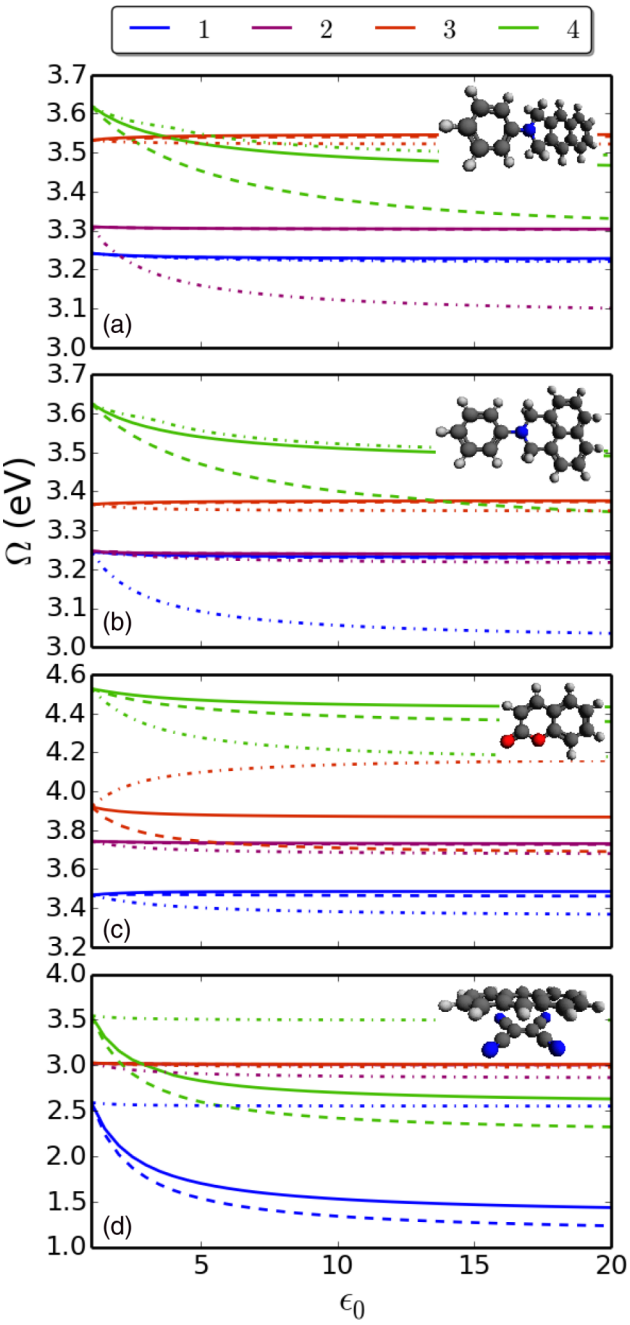

FIG. 2. Lowest four excitation energies (Ω) calculated using LR (·−), VE (−−), and SS (−) solvent models as a function of dielectric constant. For VE and SS models, each ground to ES transition is given by a different color of line and is calculated using $\bar{\mathcal{P}}_k$ such that each transition is fully relaxed within the effective solvent potential for state k. The inset shows the molecular geometry for each system with the chemical structure corresponding to (a) **1**, (b) **2**, (c) **3**, and (d) **4**/**5**.

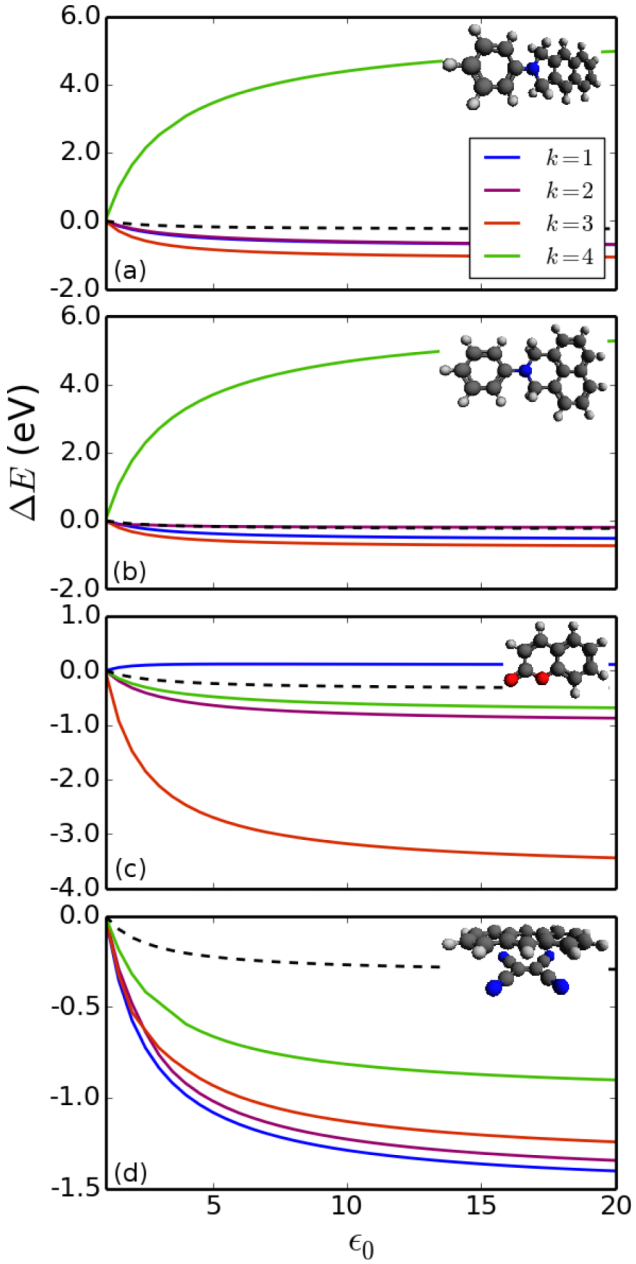

FIG. 3. Effective GS solvation energy (ΔE) for the SS model (solid) and for VE/LR (dashed) as a function of dielectric constant. For the SS model, the ΔE is given for $k = 1, 2, 3, 4$. The inset shows the molecular geometry for each system with the chemical structure corresponding to (a) **1**, (b) **2**, (c) **3**, and (d) **4**/**5**.

can be visualized using the effective GS solvent energy given by Eqs. (22) and (26) (Fig. 3) and can be discussed using the approximations of Eqs. (32) and (33). The discrepancy in the SS and VE model effects from Figs. 2(a) and 2(b), discussed above, is attributed to the destabilization of the GS for $k = 4$ in Figs. 3(a) and 3(b). These transitions have significant $\vec{\mu}_{\boldsymbol{P}} \cdot \vec{\mu}_{\boldsymbol{T}_k}$ effects such that the unrelaxed difference density and GS density have a significant interaction. A similar effect occurs due to stabilization for $k = 3$ in Fig. 2(c) and all transitions in Fig. 2(d), causing deviation between Ω for SS and VE models for the matching transitions in Fig. 2. In general, whether the effect on the GS is stabilizing or destabilizing, Ω is lower for the VE model. When this interaction is negligible, the SS and VE models predict nearly identical results. This can be seen in Figs. 4(a)-4(c), discussed below, because the corresponding plots for $k = 1$ in Fig. 3 shows the term $\vec{\mu}_{\boldsymbol{P}} \cdot \vec{\mu}_{\boldsymbol{T}_k}$ is small.

In Fig. 4, we examine the smallest four transition energies while maintaining the state $k = 1$ for SS and VE models. These calculations give the spectrum of excitation energies in the solvent potential of the first ES. In comparison to Fig. 2, where each transition k is fully relaxed in the solvent potential for ES

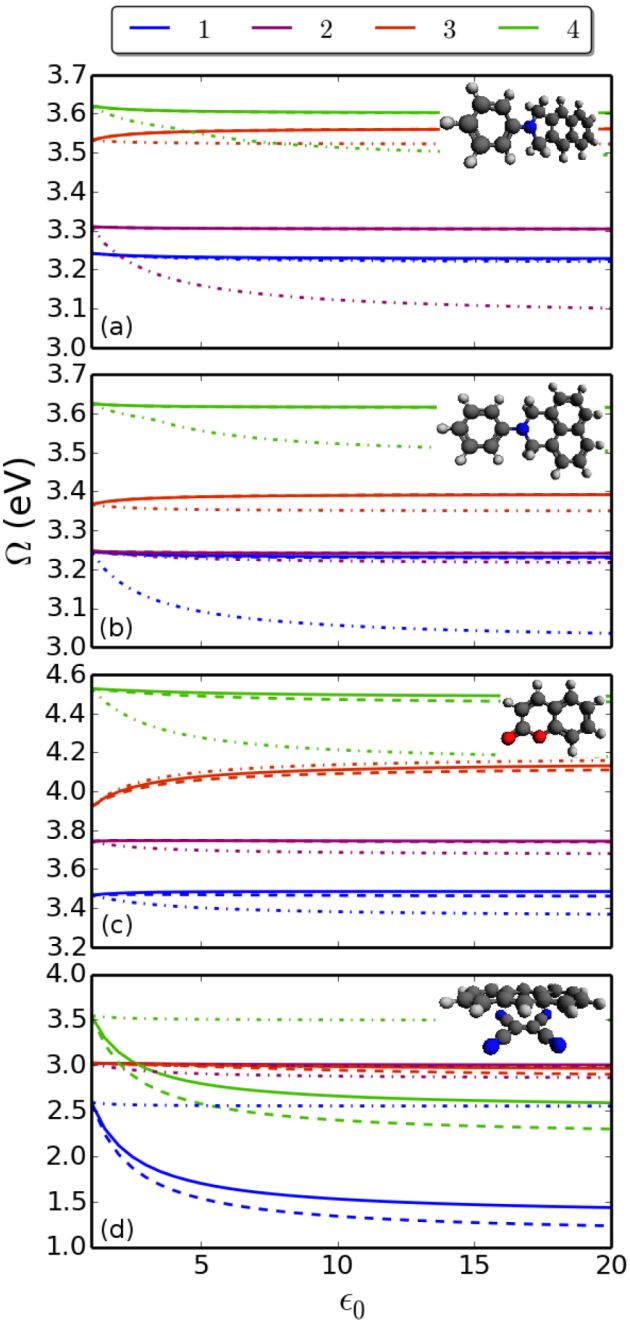

FIG. 4. Lowest four excitation energies (Ω) calculated using LR (·–), VE (––), and SS (–) solvent models as a function of dielectric constant. For VE and SS models, each ground to ES transition is given by a different color of line using $k = 1$ such that each transition is calculated within the effective solvent potential for state 1. The inset shows the molecular geometry for each system with the chemical structure corresponding to (a) **1**, (b) **2**, (c) **3**, and (d) **4**/**5**.

k, some states have drastically different shifts at given ϵ_0. These are identified as state 4 in Fig. 4(a), state 3 in Fig. 4(b), and state 4 in Fig. 4(c). The difference in solvent effect between Fig. 2 and Fig. 4 for a given molecule can be as large as the largest solvent effects in the fully relaxed case.

The interpretation of the calculations presented in Fig. 4 merits discussion. For a state to state transition, SS and VE solvent effects will reorganize the structure and possibly the ordering of the potential energy surfaces, but the transition results in a nonequilibrium solvent state. The correct application of implicit solvent would require a nonequilibrium solvent calculation[7] involving a partitioning of solvent effects from the initial solute state density and the final solute state density.

Fig. 2 shows the SS and VE solvent effects without reorganization of the solvent involved with a transition. For example, in Fig. 4(b), ΔΩ for transition 3 is increased by approximately 0.15 eV relative to the equilibrium case shown in Fig. 2(b). It is predicted that excitation in a high dielectric solvent from state 1 to 3 in the relaxed effective solvent potential of state 1 will have a larger transition energy than the corresponding transition from state 3 to state 1 in the relaxed effective solvent potential of state 3. This describes a solvation contribution to the Stokes' shift.[53]

In summary, both the SS and VE models provide similar results for ΔΩ when the interaction between the unrelaxed difference density and GS density is negligible. The deviation between the SS and VE models on the total energy thus becomes significant when this interaction is present. The LR and SS/VE models predict different effects on the transition energy, such that the LR model effect is mediated by the transition density and SS/VE model effects are mediated by the unrelaxed difference density. In general, this results in stronger SS/VE model effects on the transition energies for CT excitations.

With LR, neither the time-dependent Stokes shift nor the fluorescence solvatochromism can be described correctly because there is no effective relaxation of the solvent and ES charge density. On the other hand, correct fluorescence solvatochromism requires relaxation of the molecular structure which is not currently feasible with SS or VE models. For large systems, this requires an analytically formulated energy gradient to perform geometry relaxation. While this is easily formulated for LR,[6,94] it is not yet available within implementations of SS and VE models for TD-SCF methods. This issue will be addressed in a follow-up paper[95] and then later extended to dynamic systems.

IV. CONCLUSION

A unifying formulation of ES solvent models in TD-SCF methods has been presented. A comparison of the LR, VE, and SS models showed that CT excitations exhibit strong solvent effects in the SS and VE models, while in the LR model they generally do not. This was shown to be because the effective solvent potential is constructed from the transition density for the LR method and unrelaxed difference density for the SS and VE models. A direct comparison of the VE and SS models shows that the models predict different results for both the ground and excitation energies when the interaction of GS density and unrelaxed difference density is significant.

A follow-up publication will present the variational formulation of the ES energy and analytical gradient techniques for excited state solvent models. Then, accurate dynamic simulation methods including nonequilibrium effects will be described. Further implementations will include QM/MM methods using the presented effective solvent potentials to describe the interaction between QM and MM

systems, as well as extension to non-adiabatic dynamics in solvent.

ACKNOWLEDGMENTS

We acknowledge support of the U.S. Department of Energy through the Los Alamos National Laboratory (LANL) LDRD Program. LANL is operated by Los Alamos National Security, LLC, for the National Nuclear Security Administration of the U.S. Department of Energy under Contract No. DE-AC52-06NA25396. We also acknowledge support of the Center for Nonlinear Studies (CNLS) and the Center for Integrated Nanotechnology (CINT) at LANL. We would like acknowledge Giovanni Scalmani for useful comments on the manuscript.

APPENDIX: COSMO EFFECTIVE SOLVENT POTENTIAL

For COSMO, the effective solvent potential is defined as

$$V_S(\boldsymbol{x})_{nm\sigma} = \sum_{jk\sigma'} \langle nm\sigma|\hat{V}^S_{nm\sigma,jk\sigma'}|jk\sigma'\rangle \boldsymbol{x}_{jk\sigma}. \quad \text{(A1)}$$

$\hat{V}^S$ is a tetradic effective solvent potential operator. It may be arbitrarily defined for any continuum solvent model, such as PCM, but in this case is defined in terms of the COSMO framework of Ref. 13 to be

$$\hat{V}^S = -f(\epsilon)\Lambda^T\Theta^{-1}\Lambda. \quad \text{(A2)}$$

Summing over spin variables for brevity, the matrix elements of Θ and Λ are given by

$$\Theta_{ab} = \frac{1}{|r_a - r_b|}; \Lambda_{an} = \frac{1}{|r_a - q_n|}, \quad \text{(A3)}$$

where the position of cavity charges is given by $r_{a,b}$ and similarly for solute charges by q_n. The diagonal elements of Θ are instead parameterized by the method given in Ref. 13 along with a derivation of the dielectric scaling factor given by

$$f(\epsilon) = \frac{\epsilon + 1}{\epsilon - 0.5}. \quad \text{(A4)}$$

For the simulations in this publication, ϵ is chosen to be the static dielectric constant denoted by ϵ_0.

[1]Y. I. Park, C.-Y. Kuo, J. S. Martinez, Y.-S. Park, O. Postupna, A. Zhugayevych, S. Kim, J. Park, S. Tretiak, and H.-L. Wang, ACS Appl. Mater. Interfaces **5**, 4685 (2013).
[2]N. S. Bayliss and E. G. McRae, J. Phys. Chem. **58**, 1002 (1954).
[3]H. Lin and D. Truhlar, Theor. Chem. Acc. **117**, 185 (2007).
[4]J. Tomasi, B. Mennucci, and R. Cammi, Chem. Rev. **105**, 2999 (2005).
[5]K. Sneskov, T. Schwabe, O. Christiansen, and J. Kongsted, Phys. Chem. Chem. Phys **13**, 18551 (2011).
[6]G. Scalmani, M. J. Frisch, B. Mennucci, J. Tomasi, R. Cammi, and V. Barone, J. Chem. Phys. **124**, 094107 (2006).
[7]R. Improta, V. Barone, G. Scalmani, and M. J. Frisch, J. Chem. Phys. **125**, 054103 (2006).
[8]M. Caricato, B. Mennucci, J. Tomasi, F. Ingrosso, R. Cammi, S. Corni, and G. Scalmani, J. Chem. Phys. **124**, 124520 (2006).
[9]S. Corni, R. Cammi, B. Mennucci, and J. Tomasi, J. Chem. Phys. **123**, 134512 (2005).
[10]C. J. Cramer and D. G. Truhlar, Chem. Rev. **99**, 2161 (1999).
[11]V. Barone and M. Cossi, J. Phys. Chem. A **102**, 1995 (1998).
[12]B. Mennucci, WIREs Comput. Mol. Sci. **2**, 386 (2012).
[13]A. Klamt and G. Schüürmann, J. Chem. Soc., Perkin Trans. 2 **1993**, 799.
[14]J. Gao, J. Comput. Chem. **18**, 1061 (1997).
[15]D. Thouless, Nucl. Phys. **22**, 78 (1961).
[16]D. J. Thouless, *The Quantum Mechanics of Many-Body Systems* (Academic Press, New York, 1972).
[17]Y. Tawada, T. Tsuneda, S. Yanagisawa, T. Yanai, and K. Hirao, J. Chem. Phys. **120**, 8425 (2004).
[18]J.-D. Chai and M. Head-Gordon, Phys. Chem. Chem. Phys. **10**, 6615 (2008).
[19]T. Yanai, D. P. Tew, and N. C. Handy, Chem. Phys. Lett. **393**, 51 (2004).
[20]E. R. Davidson, J. Comput. Phys. **17**, 87 (1975).
[21]S. Rettrup, J. Comput. Phys. **45**, 100 (1982).
[22]J. Olsen, H. J. A. Jensen, and P. Jorgensen, J. Comp. Phys. **74**, 265 (1988).
[23]S. Tretiak and S. Mukamel, Chem. Rev. **102**, 3171 (2002).
[24]M. E. Casida, C. Jamorski, K. C. Casida, and D. R. Salahub, J. Chem. Phys. **108**, 4439 (1998).
[25]R. E. Stratmann, G. E. Scuseria, and M. J. Frisch, J. Chem. Phys. **109**, 8218 (1998).
[26]V. Chernyak, M. F. Schulz, S. Mukamel, S. Tretiak, and E. V. Tsiper, J. Chem. Phys. **113**, 36 (2000).
[27]S. Tretiak, C. M. Isborn, A. M. Niklasson, and M. Challacombe, J. Chem. Phys. **130**, 054111 (2009).
[28]C. F. Guerra, J. G. Snijders, G. Veldev, and E. J. Baerends, Theor. Chem. Acc. **99**, 391 (1998).
[29]S. Goedecker, Rev. Mod. Phys. **71**, 1085 (1999).
[30]E. Schwegler, M. Challacombe, and M. Head Gordon, J. Chem. Phys. **106**, 9708 (1997).
[31]M. Challacombe, J. Chem. Phys. **110**, 2332 (1999).
[32]M. C. Strain, G. E. Scuseria, and M. J. Frisch, Science **271**, 51 (1996).
[33]P. Sałek, S. Høst, L. Thøgersen, P. Jørgensen, P. Manninen, J. Olsen, B. Jansík, S. Reine, F. Pawłowski, and E. Tellgren, J. Chem. Phys. **126**, 114110 (2007).
[34]G. Galli, Curr. Opin. Solid State Mater. Sci. **1**, 864 (1996).
[35]P. Ordejón, Comput. Mater. Sci. **12**, 157 (1998).
[36]G. Scuseria, J. Phys. Chem. **103**, 4782 (1999).
[37]S. Y. Wu and C. S. Jayanthi, Phys. Rep. **358**, 1 (2002).
[38]D. Rocca, R. Gebauer, Y. Saad, and S. Baroni, J. Chem. Phys. **128**, 154105 (2008).
[39]A. F. Izmaylov, E. N. Brothers, and G. E. Scuseria, J. Chem. Phys. **125**, 224105 (2006).
[40]J. Kussmann and C. Ochsenfeld, J. Chem. Phys. **127**, 054103 (2007).
[41]X. Andrade, S. Botti, M. A. L. Marques, and A. Rubio, J. Chem. Phys. **126**, 184106 (2007).
[42]S. Coriani, S. Høst, B. Jansík, L. Thøgersen, J. Olsen, P. Jørgensen, S. Reine, F. Pawłowski, T. Helgaker, and P. Sałek, J. Chem. Phys. **126**, 154108 (2007).
[43]C. Y. Yam, S. Yokojima, and G. H. Chen, Phys. Rev. B **68**, 153105 (2003).
[44]S. Yokojima and G. H. Chen, Chem. Phys. Lett. **292**, 379 (1998).
[45]R. Improta, G. Scalmani, M. J. Frisch, and V. Barone, J. Chem. Phys. **127**, 074504 (2007).
[46]R. Cammi and B. Mennucci, J. Chem. Phys. **110**, 9877 (1999).
[47]M. Cossi and V. Barone, J. Chem. Phys. **112**, 2427 (2000).
[48]A. V. Marenich, C. J. Cramer, D. G. Truhlar, C. A. Guido, B. Mennucci, G. Scalmani, and M. J. Frisch, Chem. Sci. **2**, 2143 (2011).
[49]M. Caricato, J. Chem. Theory Comput. **8**, 4494 (2012).
[50]M. Caricato, J. Chem. Theory Comput. **8**, 5081 (2012).
[51]R. Cammi, R. Fukuda, M. Ehara, and H. Nakatsuji, J. Chem. Phys. **133**, 024104 (2010).
[52]R. Cammi, Int. J. Quantum Chem. **110**, 3040 (2010).
[53]B. Bagchi, Annu. Rev. Phys. Chem. **40**, 115 (1989).
[54]P. Ring and P. Schuck, *The Nuclear Many-Body Problem* (Springer-Verlag, New York, 1980).
[55]E. Runge and E. K. U. Gross, Phys. Rev. Lett. **52**, 997 (1984).
[56]M. E. Casida, *Recent Advances in Density-Functional Methods* (World Scientific, Singapore, 1995).
[57]S. Mukamel, *Principles of Nonlinear Optical Spectroscopy* (Oxford University Press, Oxford, 1999).
[58]A. Szabo and N. S. Ostlund, *Modern Quantum Chemistry: Introduction to Advanced Electronic Structure Theory* (McGraw-Hill, New York, 1989).
[59]S. Yokojima and G. H. Chen, Chem. Phys. Lett. **292**, 379 (1998).
[60]K. Yabana and G. F. Bertsch, Int. J. Quantum Chem. **75**, 55 (1999).
[61]A. Tsolakidis, D. Sanchez-Portal, and R. Martin, Phys. Rev. B **66**, 235416 (2002).
[62]F. Wang, C. Y. Yam, G. H. Chen, and K. Fan, J. Chem. Phys. **126**, 134104 (2007).
[63]E. K. U. Gross, J. F. Dobson, and M. Petersilka, *Density Functional Theory*, edited by R. F. Nalewajski (Springer, Berlin, 1996), Vol. 181.

[64]K. Burke, J. Werschnik, and E. Gross, J. Chem. Phys. **123**, 062206 (2005).
[65]M. Lein and S. Kümmel, Phys. Rev. Lett. **94**, 143003 (2005).
[66]A. D. Becke, J. Chem. Phys. **98**, 1372 (1993).
[67]C. J. Cramer, *Essentials of Computational Chemistry* (Wiley, West Sussex, UK, 2002).
[68]F. Furche, J. Chem. Phys. **114**, 5982 (2001).
[69]A. Graham, *Kroneker Products and Matrix Calculus With Applications* (Halstead/Wiley, New York, 1981).
[70]S. Tretiak and V. Chernyak, J. Chem. Phys. **119**, 8809 (2003).
[71]F. Furche and R. Ahlrichs, J. Chem. Phys. **117**, 7433 (2002).
[72]N. C. Handy and H. F. Schaefer III, J. Chem. Phys. **81**, 5031 (1984).
[73]T. H. Dunning and V. McKoy, J. Chem. Phys. **48**, 5263 (1967).
[74]J. Paldus and J. Čížek, J. Chem. Phys. **60**, 149 (1974).
[75]J. Oddershede and P. Jorgensen, J. Chem. Phys. **66**, 1541 (1977).
[76]J. Linderberg and E. W. Thulstrup, J. Chem. Phys. **49**, 710 (1968).
[77]R. E. Stratmann, G. E. Scuseria, and M. J. Frisch, J. Chem. Phys. **109**, 8218 (1998).
[78]S. Hirata, M. Head-Gordon, and R. J. Bartlett, J. Chem. Phys. **111**, 10774 (1999).
[79]T. H. Dunning and V. McKoy, J. Chem. Phys. **47**, 1735 (1967).
[80]J. Ho, A. Klamt, and M. L. Coote, J. Phys. Chem. A **114**, 13442 (2010).
[81]T. Nelson, S. Fernandez-Alberti, V. Chernyak, A. E. Roitberg, and S. Tretiak, J. Phys. Chem. B **115**, 5402 (2011).
[82]S. Mukamel, A. Takahashi, H. X. Wang, and G. Chen, Science **266**, 250 (1994).
[83]S. Tretiak, A. Saxena, R. L. Martin, and A. R. Bishop, Phys. Rev. Lett. **89**, 097402 (2002).
[84]S. Tretiak, V. Chernyak, and S. Mukamel, J. Phys. Chem. B **102**, 3310 (1998).
[85]S. Kilina, S. Tretiak, S. K. Doorn, Z. Luo, F. Papadimitrakopoulos, A. Piryatinski, A. Saxena, and A. R. Bishop, Proc. Natl. Acad. Sci. U.S.A. **105**, 6797 (2008).
[86]S. Kilina and S. Tretiak, Adv. Funct. Mater. **17**, 3405 (2007).
[87]T. Nelson, S. Fernandez-Alberti, A. E. Roitberg, and S. Tretiak, Acc. Chem. Res. **47**, 1155 (2014).
[88]M. J. Dewar, E. G. Zoebisch, E. F. Healy, and J. J. Stewart, J. Am. Chem. Soc. **107**, 3902 (1985).
[89]Z. R. Grabowski, K. Rotkiewicz, and W. Rettig, Chem. Rev. **103**, 3899 (2003).
[90]S. Zheng, E. Geva, and B. D. Dunietz, J. Chem. Theory Comput. **9**, 1125 (2013).
[91]R. Cammi, S. Corni, B. Mennucci, and J. Tomasi, J. Chem. Phys. **122**, 104513 (2005).
[92]M. Caricato, "Excited states: From isolated molecules to complex environments excited states," Comput. Theor. Chem. **1040–1041**, 99 (2014).
[93]M. Caricato, J. Chem. Phys. **139**, 044116 (2013).
[94]B. Mennucci, C. Cappelli, C. A. Guido, R. Cammi, and J. Tomasi, J. Phys. Chem. A **113**, 3009 (2009).
[95]J. A. Bjorgaard, V. Kuzmenko, K. A. Velizhanin, and S. Tretiak, "Solvent effects in time-dependent self-consistent field methods. II. Variational formulations and analytical gradients," J. Chem. Phys. (unpublished).